Synthesis and Characterization of a GRPR and PSMA Targeting Heterodimer for Theranostic Applications in Prostate Cancer

Job Markink
5659752

Supervisors:

Dr. Hanyue Ma, Erasmus Medical Centre, Radiopharmaceutical Chemistry
Dr. Yann Seimbille, Erasmus Medical Centre, Radiopharmaceutical Chemistry

Table of Contents

Abstract

Prostate cancer (PC) is the second most common cancer in the world for which diagnostic and therapeutic techniques require optimization. Currently the most used techniques for diagnosis are invasive digital rectal exams and blood prostate specific antigen (PSA) testing, which produces false negative and false positive results. In addition, PC overexpresses different biomarkers at different tumor stages making diagnosis and novel treatment difficult to perform. This report investigates the synthesis and characterization of PSMA and GRPR targeting heterodimers, used as a diagnostic for early and late-stage PC as well as targeted therapy. Two compounds were synthesized both containing NeoB, a PSMA targeting ligand and a DOTAGA chelator for complexing with diagnostic or therapeutic radionuclides. The platform for linking peptides utilizes a tetrazine functionality to achieve biorthogonal addition of chelators via an inverse electron demand Diels Alder (IEDDA) reaction. A cysteine on the N-terminus of the peptides allow for a biorthogonal cyano-thiol cycloaddition click reaction with the cyanopyrimidine. Two different lengths of the platform and the use of cyanopyrimidine functionalities were tested for stability. Unfortunately, the potential clinical application is limited by the poor stability of the cyanopyrimidine platform. Substituting the cyanopyrimidine functionality for tetrafluorophenyl (TFP) made the attachment of the peptides possible by increasing the stability of the platform. The reaction used to attach the peptides loses its biorthogonality but does result in the final heterodimers that can be used for further testing. The peptides were attached to a tetraflourophenyl activated platform via an amino hexanoic acid linker. Radiochemical yields and purities were determined for both final compounds.

Layman summary

Prostate cancer is the second most common cancer in the world. Techniques used for its detection and treatment thereof are far from optimal, they are either painful for the patient or don't produce correct results. New forms of detection and treatment for this disease are difficult to manufacture because the tumor does not have one target at all stages of its maturation and expansion process. This means that different medicines are needed to detect and treat the different stages. In this report the possibility of production of an all-in-one medicine is investigated. Theoretically, this molecule should be able to target all stages of prostate cancer so only one product is needed for the cancer's detection and treatment. This should increase efficiency and effectiveness of detection and treatment of prostate cancer resulting in a higher chance of patient survival. The molecule was designed in two different ways to be able to see which one is most stable in storage conditions that favor clinical applications. The first strategy introduced a certain part of a molecule that can be used for a more efficient conversion of starting materials to product but was proven to be unstable in the wanted storage conditions. Besides being stable in storage conditions, the molecule needs to stay intact when holding a radioactive metal. This radioactive metal is used for either detection or treatment of prostate cancer. The final product was also tested for stability once it was holding the radioactive metal. The version of the molecule with a shorter distance between the two targeting mechanisms seemed to have a higher stability than the longer version. However, more tests need to be done before being sure of this. Through this research an effective method of synthesis was devised for our final molecule and the products show promising results in terms of stability.

Introduction

Being the second most common cancer in the world and the fifth leading cause of death in men, prostate cancer (PC) still poses a great threat to many lives.[1] In 2020 alone, 1.4 million cases of prostate cancer were reported of which close to 30% were lethal.[2] With diagnostic techniques such as digital rectal exams and blood prostate specific antigen (PSA) testing, patients can be redirected to therapy at an earlier stage, increasing survival rate. However, these diagnostic techniques come with setbacks. The digital rectal exam is invasive and serum PSA screening has shown to produce false negative and false positive results. Between 20-30% of PC patients have serum PSA levels within the healthy range, which leads to many undiagnosed patients.[3] In addition, serum PSA levels are elevated in benign prostatic hypertrophy (BPH) and prostatitis diagnosis, resulting in unnecessary biopsies and at times unnecessary treatment.[4,5,6]

Besides diagnostic limitations, therapy for PC patients is also not optimal. The most commonly used PC treatment is chemotherapy, but due to its non-specific targeting, it also causes damage to healthy cells, resulting in dreadful side effects. Including, immunosuppression, nausea and vomiting, hair loss, infertility, etc.[7] Targeted cancer therapy is a promising and growing field within cancer treatment research. This concept takes advantage of an overexpressed protein on the cancer cell and the molecule is designed to mimic the proteins ligand (Figure 1). Due to the specific binding capabilities, it will predominantly bind to the tumour cells and drastically decrease the damage to healthy cells.[8] Currently, the biggest players in targeted cancer therapy are monoclonal antibodies. Their high specificity allows them to deliver cytotoxic agents to the tumour cells efficiently.[9] However pharmacokinetic optimization of antibodies, in terms of clearance, heterogenous tumour uptake and immunogenicity, is still a challange.[10] Recently targeted cancer therapy is slowly moving towards the use of therapeutic peptides. Therapeutic peptides are small sequences of amino acids (AAs) that are usually organised in the same way as the binding site of the target protein ligand. The advantages of therapeutic peptides are that they are small in size, have high
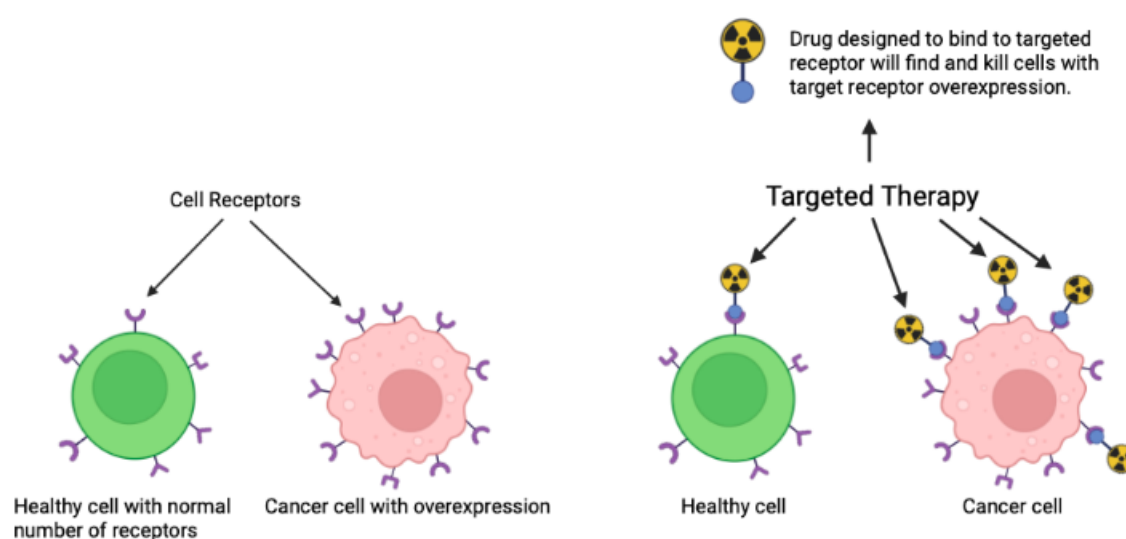

Figure 1. Targeted therapy mimics the ligand that binds to the specific receptor(s) overexpressed by cancer cells causing damage and ultimately apoptosis in cancer cells. The concentration of the drug that binds to healthy cells is too low to cause damage due to the low or undetectable expression of targeted receptor(s) compared to the cancer cells.

affinity and specificity towards its target, minimal drug-drug interactions and have relatively low liver and kidney accumulation.[11]

Attachment of a radionuclide to the peptide achieves a promising molecule for theranostic applications. Depending on the radionuclide that is attached, the molecule can be used for both diagnostic and therapeutic purposes. With the use of gamma-emitters such as ^{111}In or ^{18}F, the molecule can be used for SPECT or PET imaging respectively.[12] Alpha and beta emitters like [225]Ac or ^{68}Ga have higher energy to damage cells when internalised (targeted intracellular therapy) or brought close enough to the membrane (targeted extracellular therapy). Beta emitters have a longer range which is useful for large sized tumours but are more unpredictable in terms of side-effects.[13] Alpha emitters produce high density ionizations along a linear path causing unrepairable double-stranded breaks in the DNA of the cell, but their short range make it difficult to determine a therapeutic dose (Figure 2).[13]
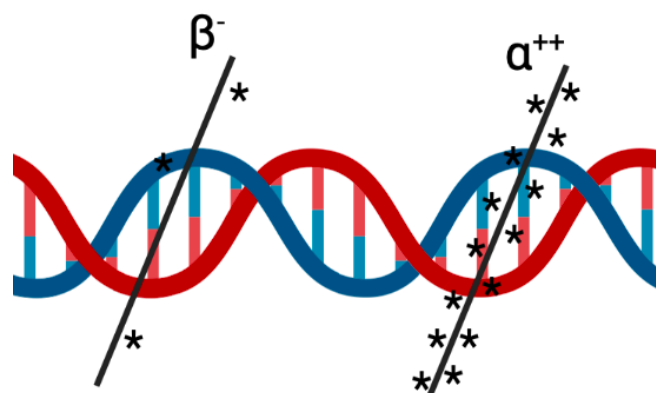

Figure 2. Difference in ionization energy between α and β emitters giving rise to their different therapeutic characteristics.

Developments in PC research have led to the discovery of two promising disease biomarkers. Prostate specific membrane antigen (PSMA) is a type II membrane protein associated with prostate cell proliferation and survival and has increased expression in prostate cancer cell lines.[14] PSMA inhibitors show great potential in terms of specificity and affinity towards PSMA and certain variations are being used for clinical diagnostics and therapeutics.[15] The expression levels of PSMA are proportional to prostate cancer stage. Later stages of PC, that are androgen-independent, express more PSMA and vice versa.[16] Gastric-releasing peptide receptor (GRPR) is a 7-part transmembrane protein containing G-protein coupled receptors.[17] GRPR is expressed in many different tissues such as the pancreas, stomach and brain. Overexpression of GRPR is associated with prostate cancer cell proliferation and survival as well. However, higher levels of overexpression are seen in androgen-dependent early stages of PC.[18] Varying levels of biomarker overexpression complicate imaging and treatment, as different diagnostic and therapeutic molecules are needed depending on the PC stage. This project aims to develop novel heterodimers equipped with both PSMA and GRPR targets that can be used for imaging and treatment of early and late-stages of PC to enhance patient survival.
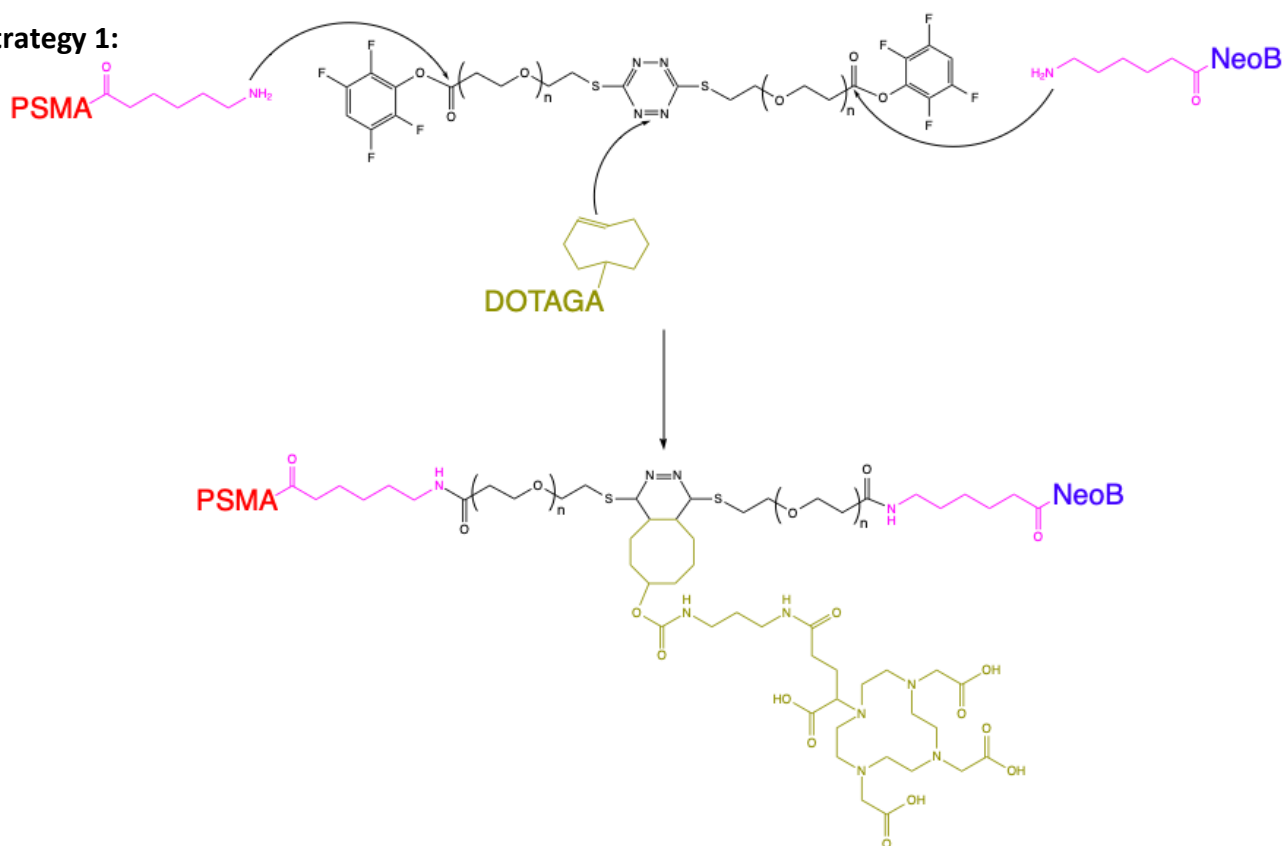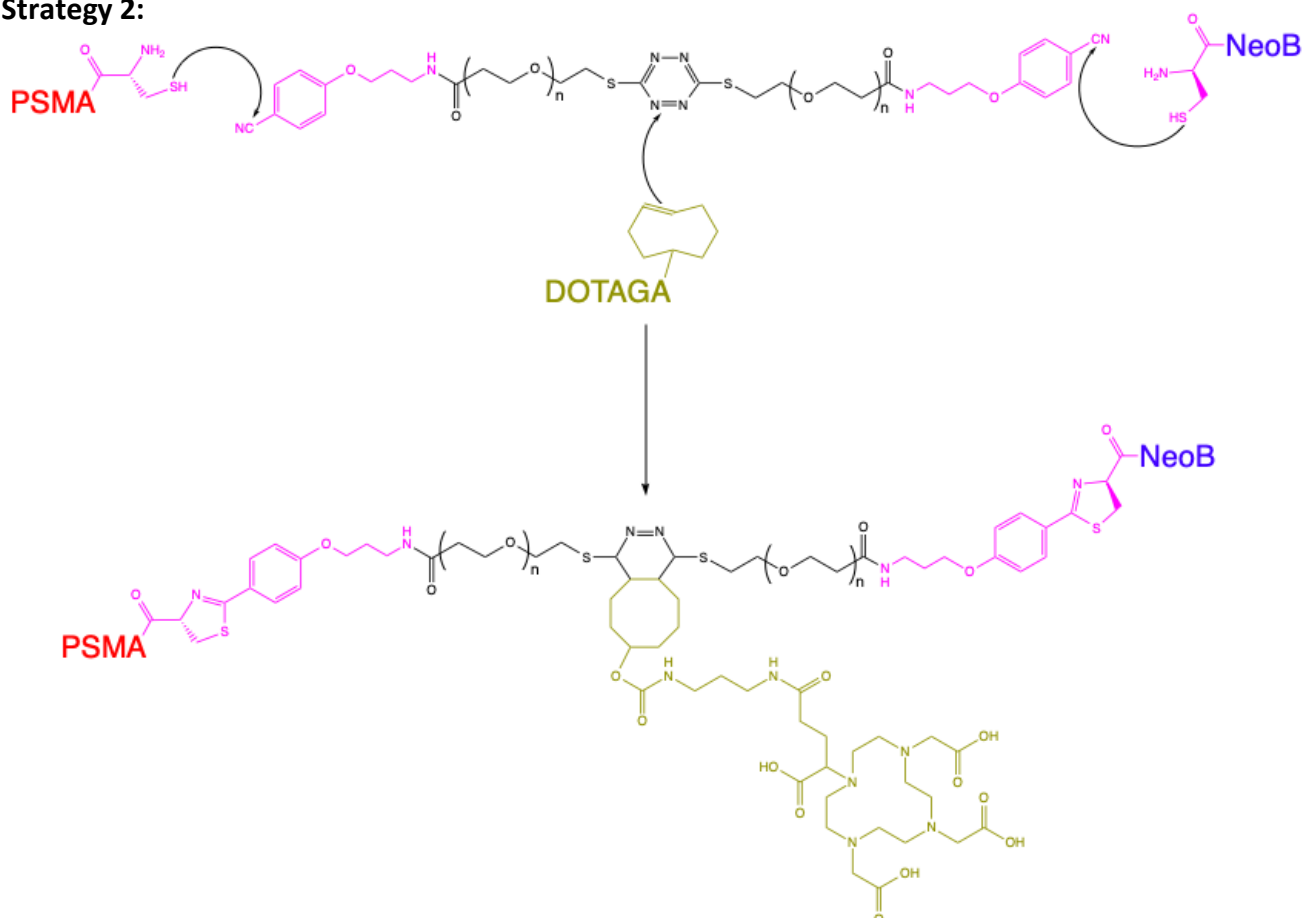
Figure 3. Two molecules designed for heterodimer synthesis. In red the PSMA targeting ligand, in blue the GRPR targeting ligand, in pink the difference between the two designs, in black the heterodimer platform and in beige the chelator.

Two potential strategies have been devised for the synthesis of the PSMA-GRPR targeting heterodimer (Figure 3). The heterodimer will consist of four separate parts: a GRPR targeting ligand, a PSMA targeting ligand, a chelator and a linkage platform. NeoB, one of the leading peptides for GRPR targeting treatment (Figure 4), will be used for targeting GRPR.[19] A newly designed ligand, still in the development phase at the Erasmus Medical Center, will be used for targeting PSMA (Figure 4). Results for target affinity and kidney uptake are promising relative to other PSMA targeting ligands used in the clinic, like PSMA-617.
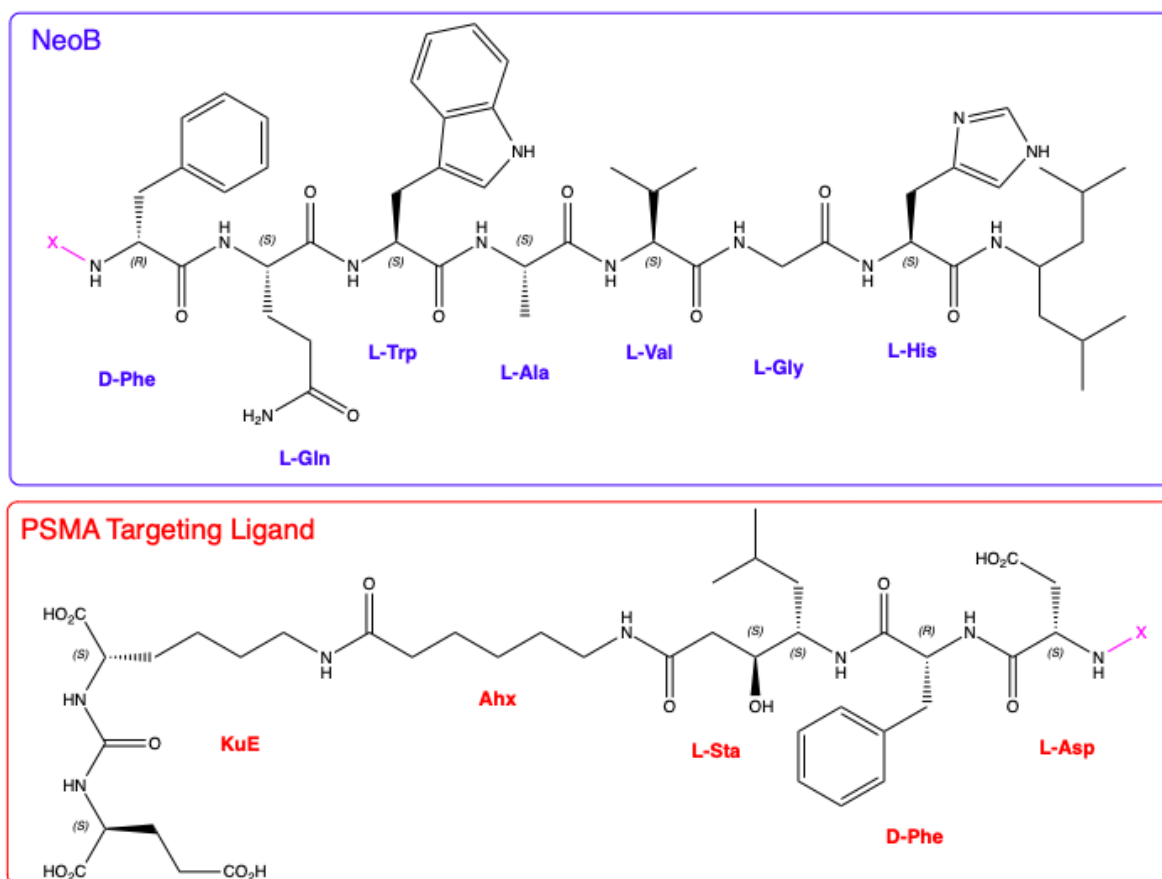

Figure 4. Structure of PSMA targeting ligand (top) and NeoB (bottom). X = D-Cys or 6-Ahx.

DOTAGA is a widely used chelator used to complex the radionuclide and is reliable when it comes to forming stable complexes with metals.[20] Compared to DOTA, the extra carboxylic acid group on DOTAGA can form an extra hydrogen bond with the radiometals, improving stability of the complex and giving the final heterodimer more hydrophilicity.[21] Finally, attachment of peptides and chelator can be achieved by coupling to a linker platform. The platform will contain a tetrazine functionality which can be used to attach chelators or fluorescence dyes through the biorthogonal inverse electron demand diels alder (IEDDA) reaction (Figure 5).[22] The reaction between a diene and tetrazine is efficient, clean and can be done in biological environments.[23]

Attached to the tetrazine is a PEG linker which can be variable in length. A longer PEG linker isolates the peptide and decreases the chance of a lowering in peptide affinity due to steric hindrance from the platform or the other peptide. However, a longer linker distance increases the risk of stability issues due to folding of the PEG. Therefore, two different lengths of PEG (PEG4, PEG8) were selected for further characterization and evaluation. The differences between the two strategies lies in the attachment of the ligands to the platform.
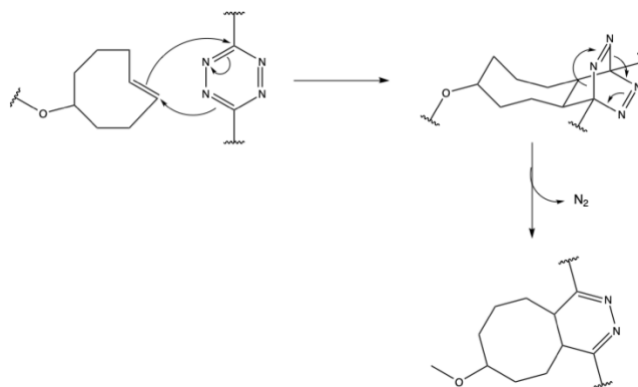
Figure 5. Mechanism of IEDDA.

In strategy 1 a cyanopyrimidine functionality is attached to the PEG linker to be used in an efficient cycloaddition reaction. The peptides will be equipped with an N-terminal cysteine which is involved in the biorthogonal cyano-thiol cycloaddition reaction.[24] However we are concerned for the stability of cyanopyrimidine in aqueous environments. Therefore, a second strategy is proposed where the cysteine on the ligands is replaced by an amino hexanoic acid linker which will be coupled directly to the carboxylic acid on the PEG linker through amide bond formation. To improve the efficiency and selectivity of this reaction the carboxylic acid on the PEG is pre-activated with a terafluorophenyl (TFP) group. The use of TFP esters has two advantages: first risk for hydrolysis under basic conditions is lower. Second, it allows the coupling of the PSMA ligand first, improving the solubility of the intermediate product, due to the presence of its free carboxylic acid moieties.[25]

Results & Discussion

Strategy 1: Synthesis, characterization and stability testing

A Boc protected amine group was introduced to the cyanopirimidine moiety through Sn2 nucleophilic substitution (Scheme 1). Acetone was used as solvent as to follow the Finkelstein reaction mechanism.[26] Alkyl bromides convert to alkyl iodides through an equilibrium reaction when in the presence of NaI. Reaction equilibrium is shifted towards the alkyl iodide when acetone is used a solvent due to the insolubility of the resulting NaBr in acetone. The slight acidity of the hydroxyl group on the cyanopirimidine moiety makes it a good nucleophile and with K_2CO_3 as a drying agent the reaction has a high efficiency when performed under reflux. Flash column chromatography deemed to be an efficient way to purify compound **1**, as can be seen in the liquid chromatography (LC) chromatogram (Figure 7).

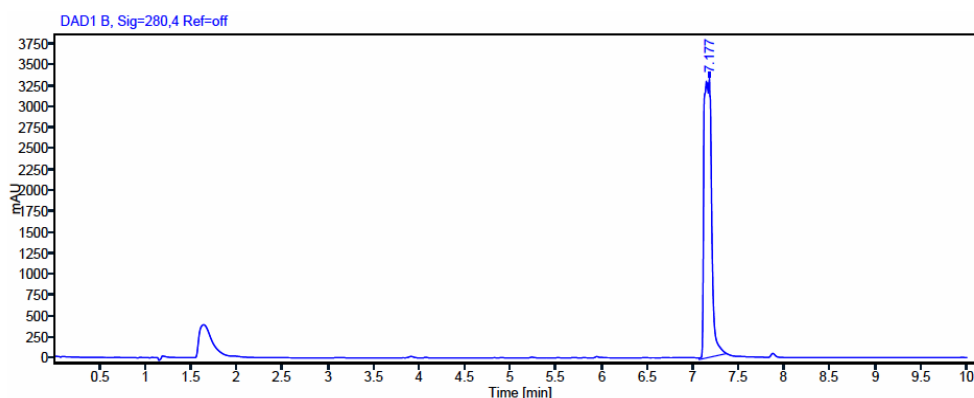**Scheme 1.** Reaction scheme for introduction of Boc protected amine.

Figure 7. *LC* chromatogram of **1** (t_R = 7.177 min).

To free the amine for subsequent conjugation of the PEG linker, the acid labile Boc protecting group was removed through TFA cleavage (Scheme 2). Cleavage of the Boc protecting group is a fast reaction and happens spontaneously at room temperature.[27] If left to react for too long the reaction could reverse and the Boc groups could reattach to the amine. Thioanisole is therefore used as a Boc protecting group scavenger and prevents this reattachment. The free amine on compound **2** made it difficult to purify the compound through flash column chromatography, so reverse phase High Pressure Liquid Chromatography (HPLC) was used for purification instead and proved to be efficient in removing side products (Figure 8).
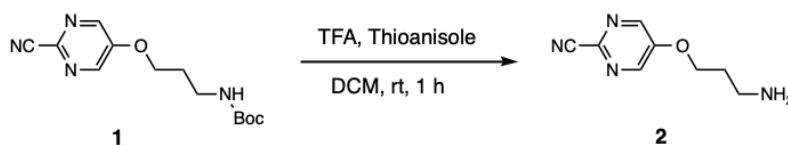
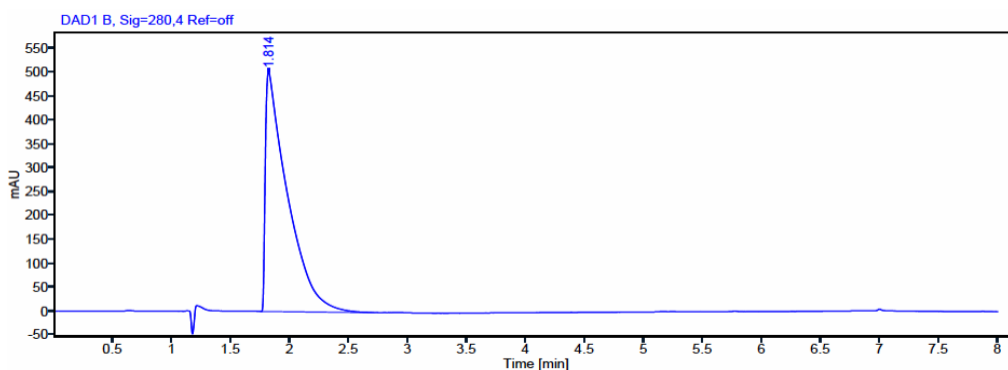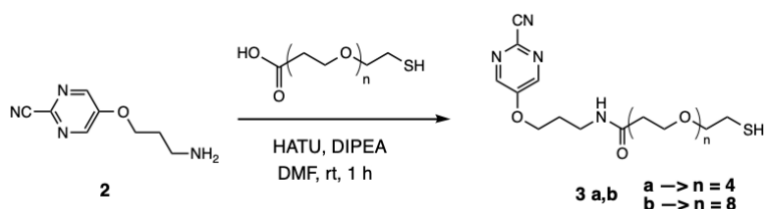**Scheme 2**. Reaction scheme for Boc cleavage.

Figure 8. LC Chromatogram of **2** (t_R = 1.814).

Both PEG$_4$ and PEG$_8$ linkers were coupled to the cyanopirimidine functionality in parallel through amide bond formation in the presence of HATU and DIPEA as base (Scheme 2).[28]

Scheme 3. Reaction scheme for amide bond formation.

Compounds **3a** and **3b** were both purified through HPLC (figure 9). Surprisingly low yields were seen after purification of both compounds (17% for **3a**, 6% for **3b**). The lower yield seen for **3b** compared to **3a** is due to the increasing length of the PEG$_8$ linker. Folding of the linker decreases its reactivity and a long linker has a higher chance of folding. Even though it is unclear why the overall yield for both compounds are low, we believe it is due to the free thiol interfering in the amide bond formation in some way. Enough product was synthesised to continue with dimerization of both compounds.
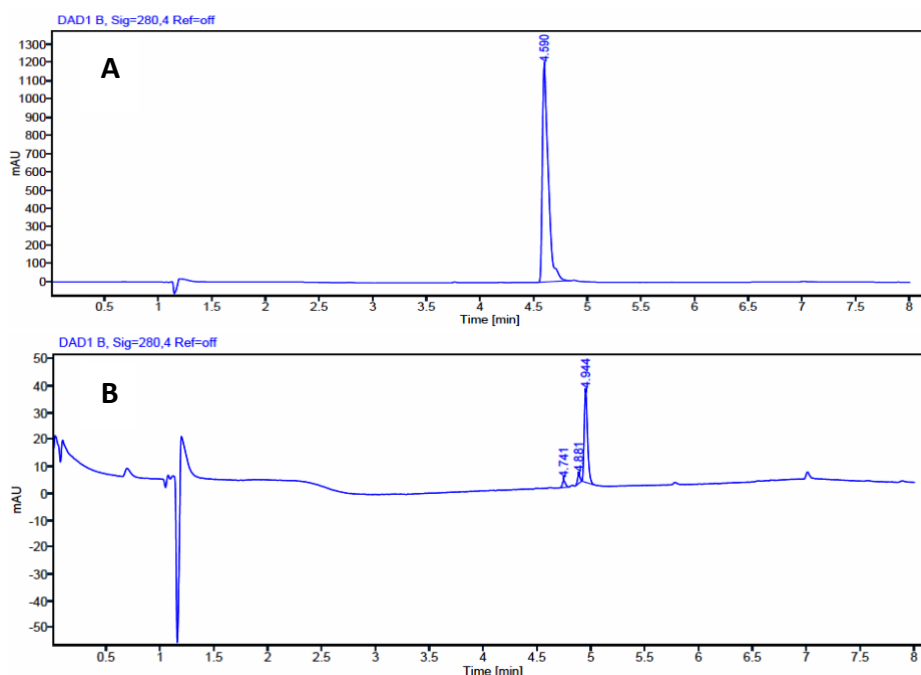

Figure 9. A) LC chromatogram of **3a** (t_R = 4.590). B) LC chromatogram of **3b** (t_R = 4.944).

To create a dimerized platform the synthesized cyanopirimidine compound was reacted with 3, 6-dichloro-1, 2, 4, 5-tetrazine. Two tertiary alkyl halide moieties on the tetrazine favour Sn1 nucleophilic substitutions in the presence of a base (Scheme 4).[29] The disubstitution is favoured by using at least 2 equivalents of the cyanopirimidine compound compared to the tetrazine. The reaction was protected from light because tetrazine, and derivatives thereof, show stability issues when exposed to light.
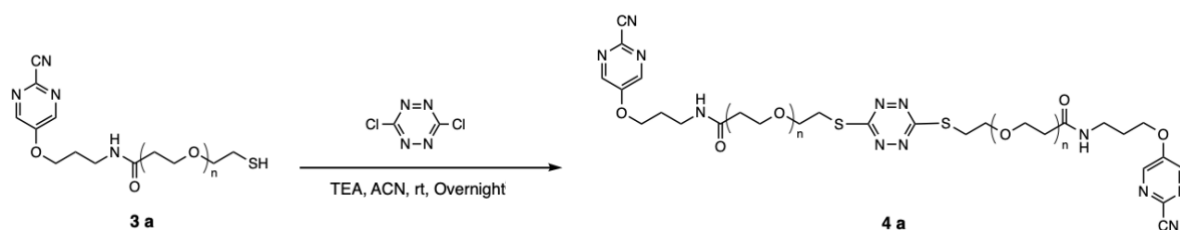
Scheme 4. Reaction for dimerisation with tetrazine.

This reaction also produced a low yield (4%) so, to have an efficient synthesis of the final compound, the last two steps of the synthesis scheme were optimized. In the amide bond formation reaction, the lower yield can be explained by steric hindrance through folding of the long PEG molecule. Furthermore, the PEG linkers contain an unprotected thiol group which can interfere with the reactivity of the carboxylic acid in the coupling reaction. When working with acid-PEG-thiol there have been reported cases of using pre-activated carboxylic acids or coupling the thiol primarily.[30] Protecting the thiol with an acid labile protecting group such as a Boc or a trityl is an option as well, but adds extra steps to the synthesis. Therefore, reacting the thiol group first could be more advantageous. During dimerization of the tetrazine, the thiol will undergo an Sn2 nucleophilic substitution with an aromatic chlorine. The weaker nucleophilicity of the carboxylic acid compared to the thiol will not interfere and the substitution of the chlorine with the thiol is favoured. This reaction between dichloro tetrazines and thiols is often used in the stapling and cyclization of peptides by using phase transfer conditions (Figure 9).[31] The PEG linkers are soluble in water and dichloro tetrazine is soluble in organic solvents. With the addition of a base, which deprotonates the thiol and creates the thiolate nucleophile, the linker reacts with the tetrazine through vigorous stirring and produces a dimer that is soluble in water. The red colour of the tetrazine will therefore shift from the organic to the aqueous phase confirming the completion of the reaction.[31]
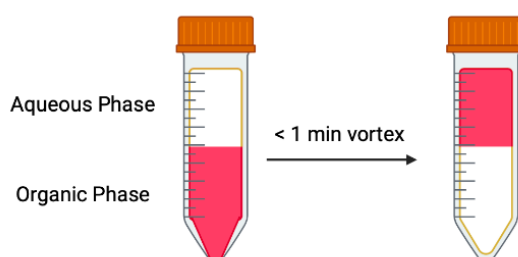
Figure 10. Phase transfer reaction showing the change in colour once the tetrazine (in organic phase before mixing) reacts with the compound in the aqueous phase.

To optimize the synthesis route, the acid-PEG-thiol linkers were attached to the tetrazine through phase transfer (Scheme 5). The PEG containing compound was used in excess (3 equivalents) to favour dimerization of the tetrazine. The phase transfer reaction proved to be clean and did not leave side products in the aqueous phase (Figure 11). No purification was needed after this step.
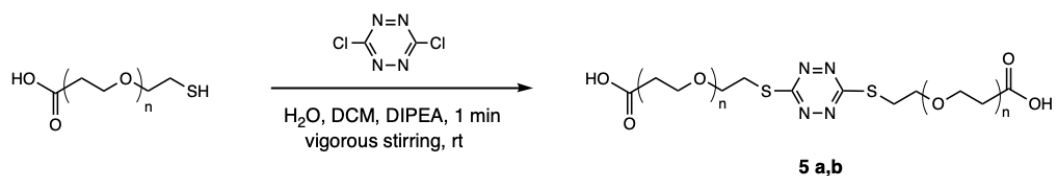
Scheme 5. *Reaction scheme for dimarization through phase transfer.*
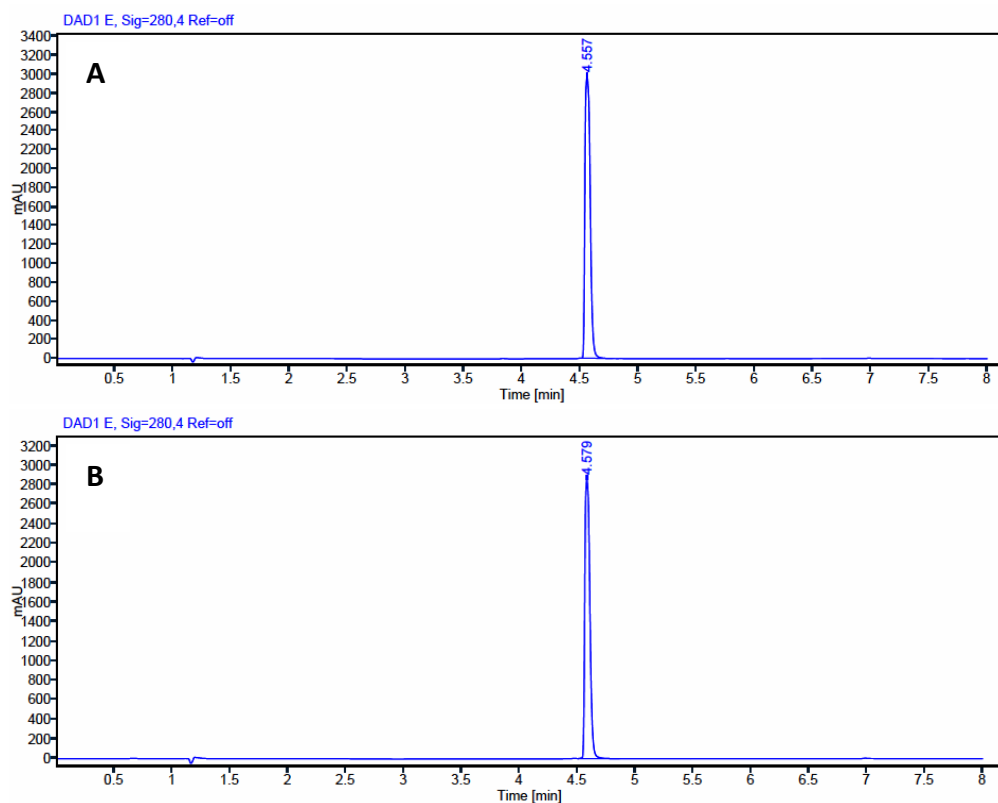
Figure 11. A) LC chromatogram of **5a** (t_R = 4.557). B) LC chromatogram of **5b** (t_R = 4.579).

Compound **2** was then attached to the dimer through amide bond formation using the same conditions as for the synthesis of **3a** and **3b**. After purification through HPLC (Figure 12) yields were calculated and compared to the percentage yields gotten through the first synthesis pathway. With significant improvement of the yields, from 17% to 58% in the first step and 4% to 26% in the second step, the optimized route was used in further synthesis of this platform.
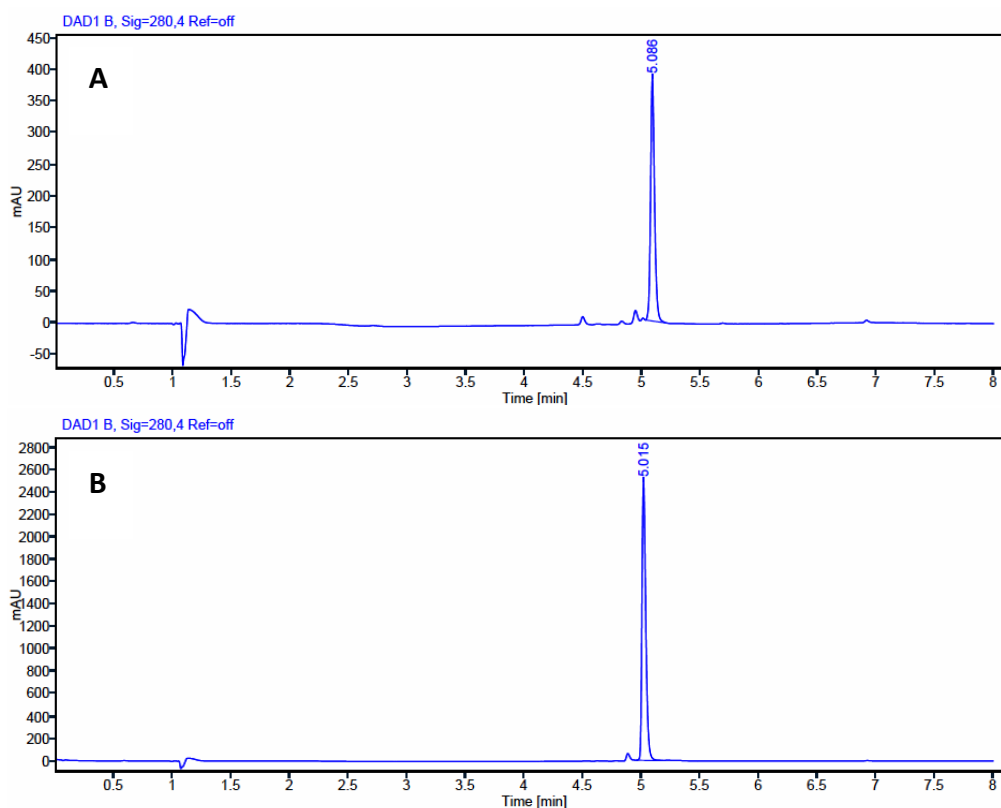
Figure 12. A) LC chromatogram of **4a** (t_R = 5.086). B) LC chromatogram of **4b** (t_R = 5.015).

To ensure that the linkage formed through cycloaddition is stable, we mimicked the attachment of a peptide through the addition of a cysteine amino acid. As the PEG$_8$ variation of the platform is theoretically more unstable than the PEG$_4$ variant from proving stability of the PEG$_8$ variant it can be assumed that the PEG$_4$ variant is stable too. The platform needs be stable in the acidic conditions used to radiolabel the final heterodimer which is why these same labelling conditions are used for testing the stability. Heating at 90°C speeds up the complexing of the radionuclide and the chelator. Addition of DTPA after heating scavenges the remaining non-complexed radionuclide. A hydrochloric acid solution (0.05 M) is used to mimic the pH of the radionuclide used during radiolabelling. This stability test performed before the radioactive labelling ensures that decomposition of the heterodimer can be distinguished due to radio radicals. Unfortunately, after heating and addition of DTPA formation of multiple peaks around the product peak showed that the heterodimer decomposed (Figure 14a,b). The stock solution of the compound dissolved in water was checked after 3 hours, the impurity peaks were growing over time (Figure 14c). These results show that the unstable characteristics of the cyanopyrimidine are too prominent to be used in the design of the PSMA and GRPR targeting heterodimer.
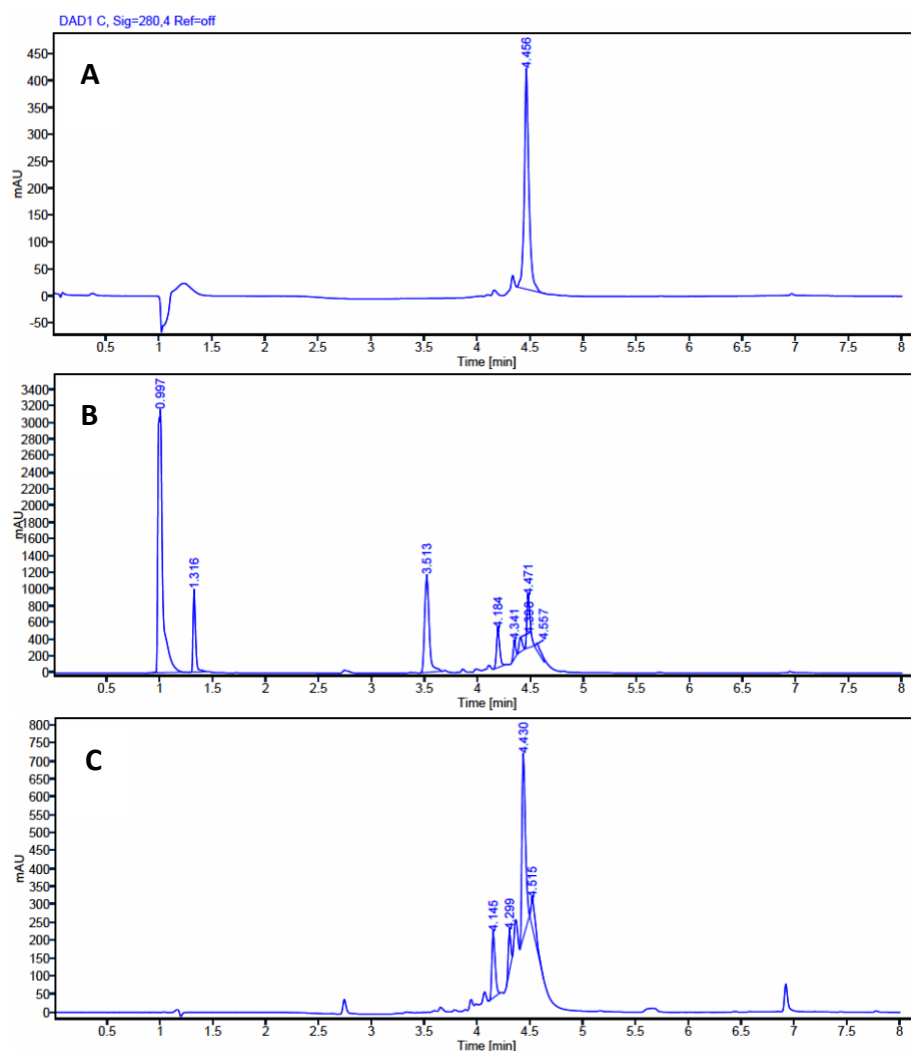
Figure 13. Stability study of compound **6** by using LC-MS. A) Compound **6** pure. B) Compound **6** under labelling conditions after 20 min of heating at 90°C. t_R = 0.5-4 min correspond to labelling matrix compounds. C) Compound **6** decomposed after 3 hours incubation at room temperature in water.

Strategy 2: Synthesis, characterization and stability testing

The biorthogonal cyano-thiol cycloaddition in strategy one is substituted by an amide bond formation in strategy 2 which was designed to solve the stability problem by avoiding the use of cyanopyrimidine. Compounds **5a** and **5b** were subjected to carboxylic acid activation through esterification with TFP. TFP is a much better leaving group than a hydroxyl moiety and therefore increases the efficiency of the subsequent amide bond formation with the two peptides. DIC was used as coupling agent for the esterification of the carboxylic acid resulting
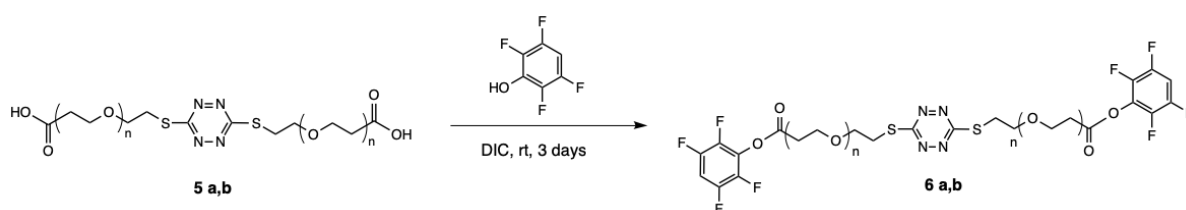
Scheme 6. *Reaction scheme for TFP activation.*

in compounds **6a** and **6b** (Scheme 6).[32] The reaction proved to be very slow and temperatures could not be highered due to instability of the TFP ester. Hydrolysis of **6a** and **6b** was noticed after HPLC purification which is due to the aqueous eluents used. TFP activated carboxylic acids are susceptible to hydrolysis in acidic and basic aqueous environments. To minimize the amount of hydrolysis extraction with water and DCM was performed to avoid HPLC purification and showed great efficiency in removing coupling agents, monosubstituted TFP impurities and starting material **5a** and **5b** (Figure 14).
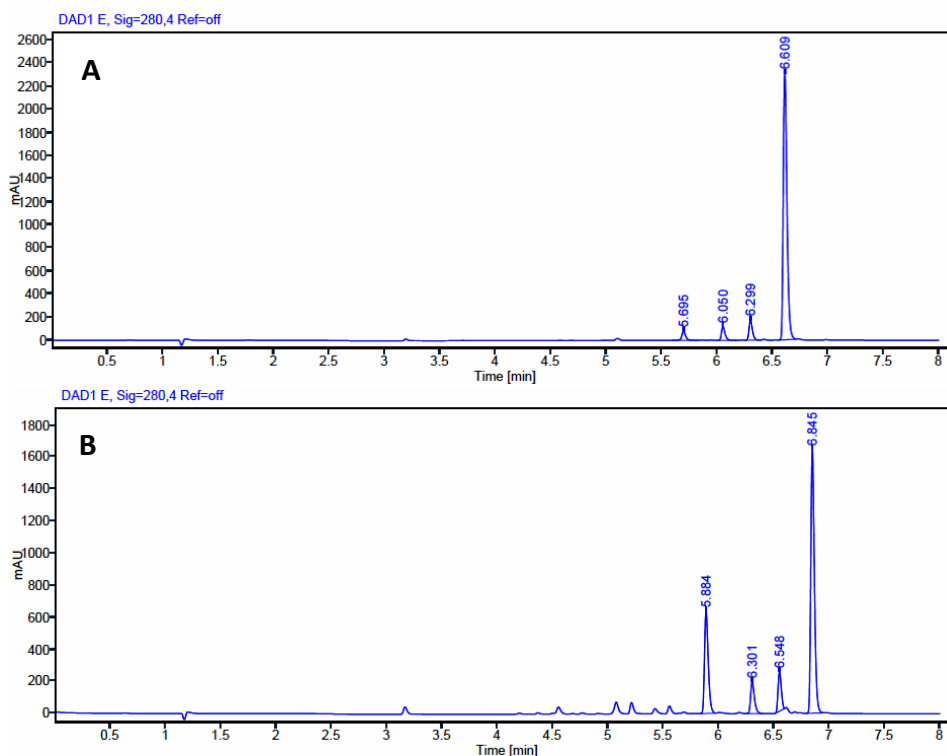

Figure 14. A) LC chromatogram of **6a** (t_R = 6.609). B) LC chromatogram of **6b** (t_R = 6.845).

The PSMA and GRPR targeting ligands were synthesised in parallel through Fmoc solid phase peptide synthesis (SPPS). The glutamic acid-uredo sequence on the PSMA targeting ligand, which when attached to lysine is the binding moiety and gives the ligand its high affinity, is synthesized separately in solution (Figure 15A). The purified product is then coupled to the N-terminal of the ivDde protected lysine pre-loaded on resin. Deprotection of the ivDde was performed with 5% hydrazine in DCM which proved to be a long and difficult reaction to push to completion. After 7 hours it was decided to continue with the elongation of the peptide even though not all ivDde was deprotected. The use of a higher hydrazine concentration could be attempted in future PSMA targeting ligand synthesis, but this increases the risk of peptide decomposition. Elongation of the peptide was performed by Fmoc deprotection of each amino acid with 20% piperidine in DMF and subsequent coupling of the following amino acid with Oxyma/HBTU and DIPEA. Full conversion of deprotection and coupling steps were checked using the Kaiser test and TNBS test. The coupling of the amino hexanoic acid to a phenylalanine was slow with milder coupling reagents, which could be explained by the steric hindrance the phenylalanine provides. Therefore, HATU and DIPEA were used for this coupling reaction. Purification by HPLC deemed to be successful at isolating the PSMA targeting ligand (Figure 15B).
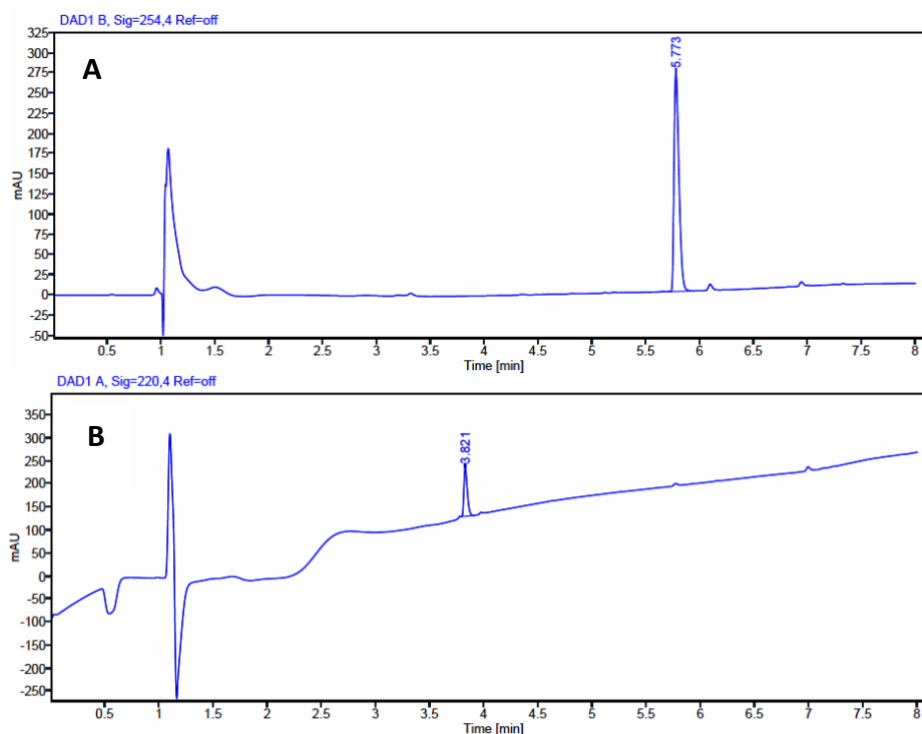
Figure 15. A) LC chromatogram of glutamic acid-uredo sequence (t_R = 5.773). B) LC chromatogram of PSMA Targeting Ligand (t_R = 3.821).

Synthesis of NeoB followed a similar Fmoc protected SPPS protocol as PSMA targeting ligands. During the synthesis of NeoB it was noticed that the size of the reaction vessel has a maximum allowed resin amount for efficient coupling and deprotection of amino acids. In a 15mL reaction vessel 133 mg of resin showed positive Kaiser and TNBS tests after coupling and negative tests after deprotection. Therefore, the amount of resin in the reaction tube was halved to allow for more efficient deprotection and coupling. After coupling of the final amino acid, the peptide was cleaved with HFIP to obtain a fully protected peptide with a free C-terminus which can be coupled with the hydrophobic C-terminal that functions as binding moiety of NeoB. However, once the C-terminal is coupled the final product is too hydrophobic to be analysed by LC-MS. Therefore, a small portion of the reaction mixture is dried and deprotected with TFA to confirm product formation by LC-MS. Purification was done through HPLC (Figure 16).
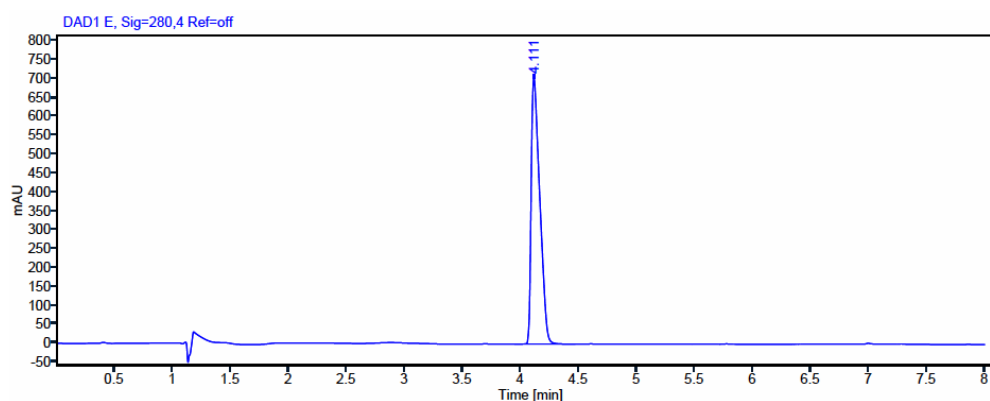
Figure 16. LC chromatogram of NeoB (t_R = 4.111).

Compound **6a** and **6b** were used to form a link between the two peptides in a one-pot reaction (Scheme 7).[33] PSMA was added to the reaction mixture where **6a** and **6b** were added in excess (1.5 eq.) to favour the formation of the monosubstituted PSMA intermediate. The reaction was left for not more than 30 min before the addition of NeoB because the hydrolysis **6a** and **6b** proved to be challenging to control under basic conditions. NeoB was added to obtain the heterodimers **7a** and **7b** after HPLC purification (Figure 17). Finally, **7a** and **7b** were subjected to the click reaction with TCO-DOTAGA[34] which efficiently produced final products **8a** and **8b** after HPLC furification (Figure 18).
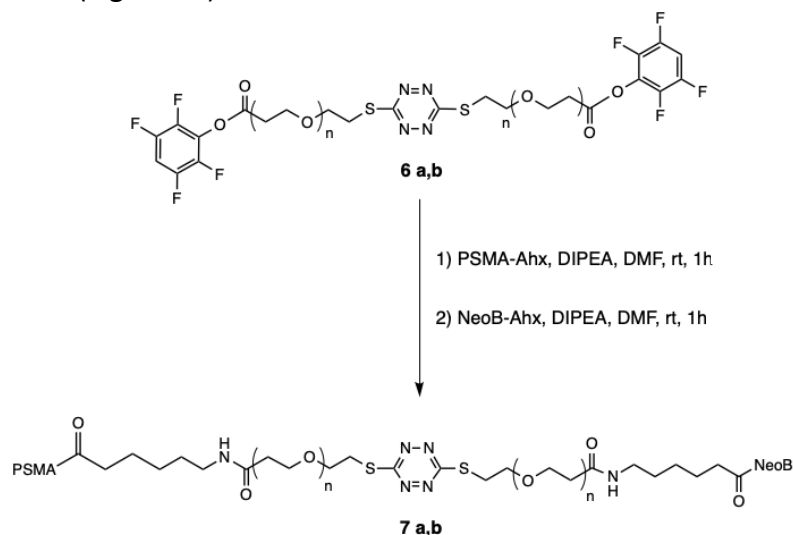
Scheme 7. *Reaction scheme for peptide attachment.*
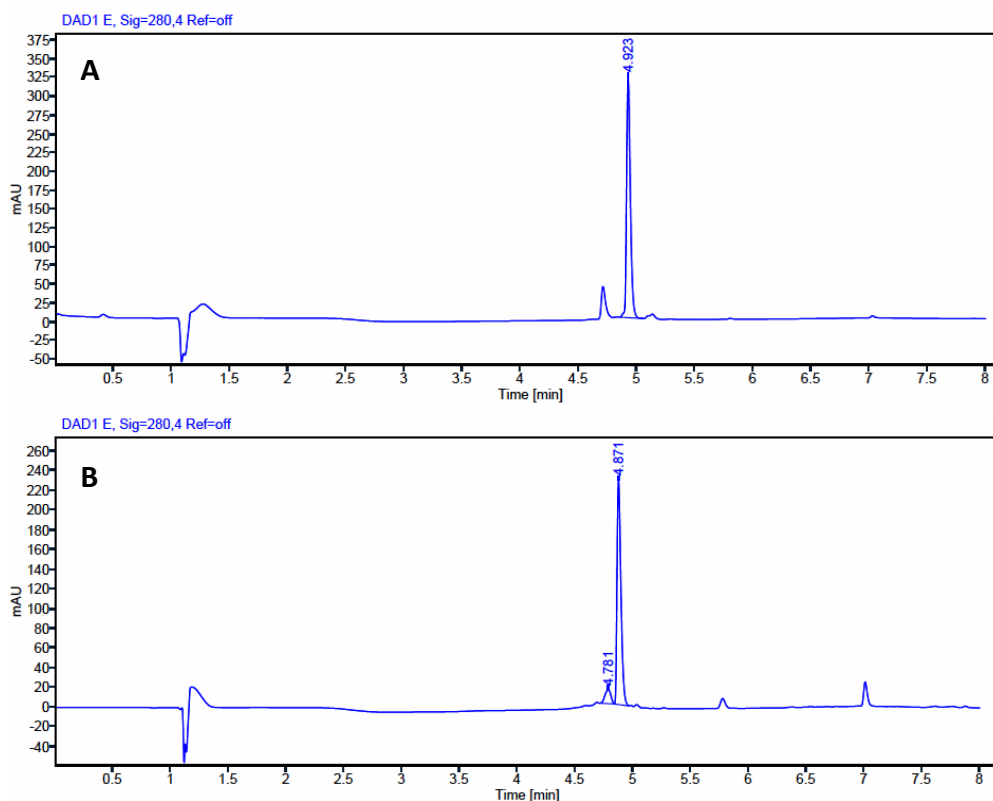
Figure 17. A) LC chromatogram of **7a** (t_R = 4.923). B) LC chromatogram of **7b** (t_R = 4.871).
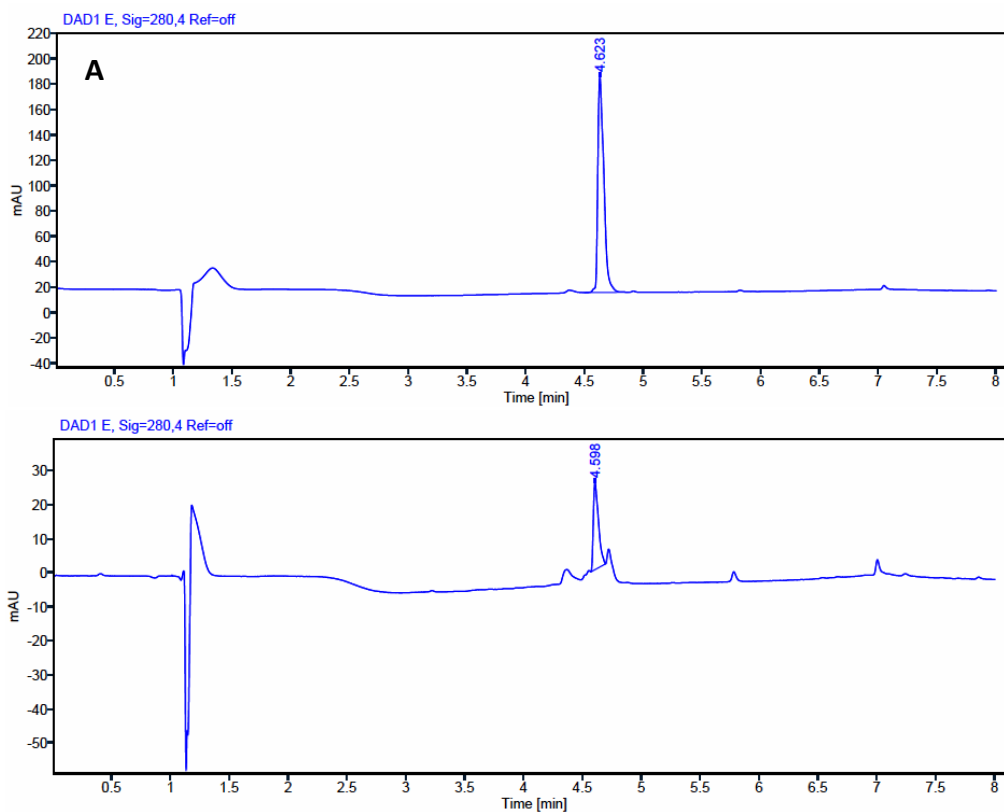
Figure 18. A) LC chromatogram of **8a** (t_R = 4.623). B) LC chromatogram of **8b** (t_R = 4.598).

Stability study of the final heterodimer **8b** was conducted following the same protocol as in strategy 1. The stability of compound **8b** was monitored after 20 min of heating in labelling matrix then incubated at room temperature and checked at different time points (3 h, 44 h) (Figure 19). All chromatograms remained as one major peak corresponding to the compound. Stability of **8b** under labelling conditions was confirmed. As this is the PEG_8 which theoretically is more unstable variation, **8a** was assumed to be stable under labelling conditions too and were both carried through to radiochemical yield and purity testing.
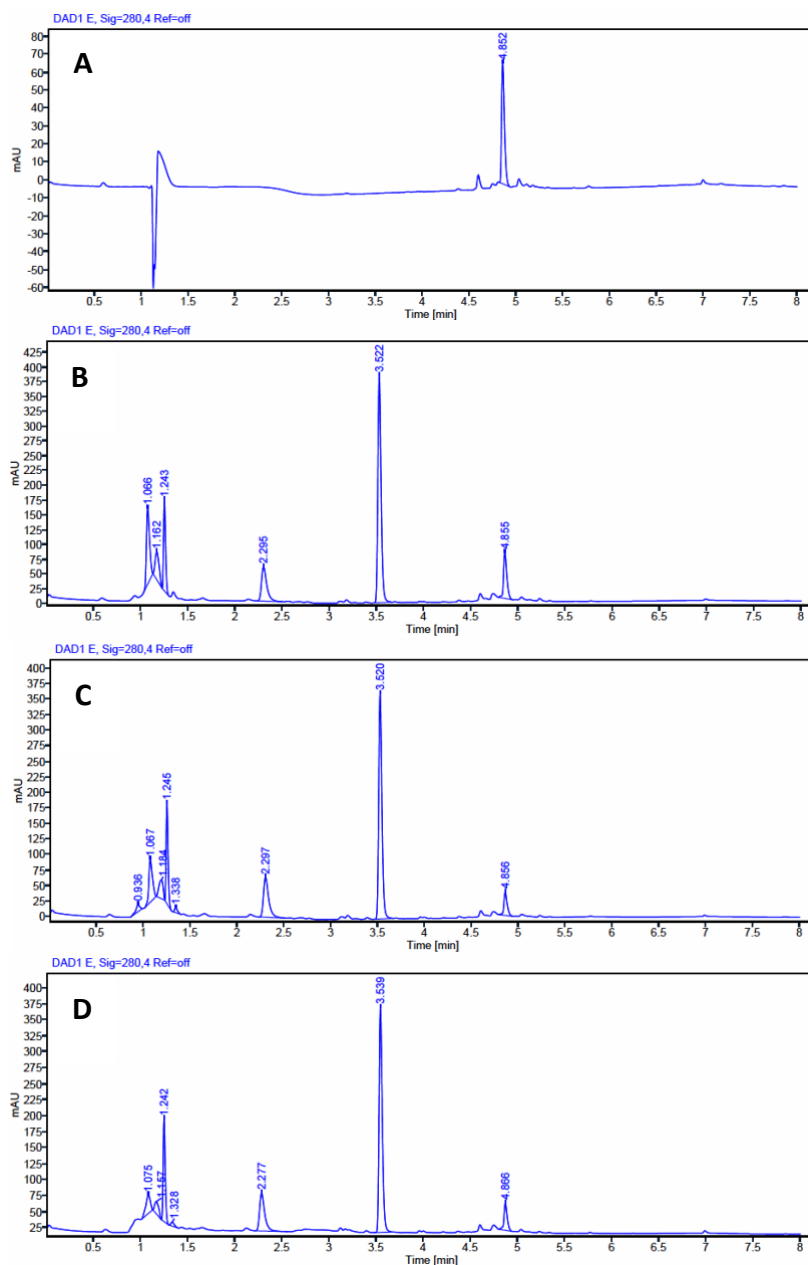
Figure 19. Stability testing chromatograms compound **8b**. A) Compound **8b** at t=0.
B) Compound **8b** under labelling conditions after incubation at 90°C in water for
20 min. Peak at retention time 4.855 min corresponds to the compound. The
peaks from 0.5-4 min correspond to labelling matrix compounds. C) Compound **8b**
under labelling conditions incubated at rt for 3 hours. Peak at retention time 4.856
min corresponds to the compound. The peaks from 0.5-4 min correspond to
labelling matrix compounds. D) Compound **8b** under labelling conditions incubated
at rt for 44 hours. Peak at retention time 4.866 min corresponds to the compound.
The peaks from 0.5-4 min correspond to labelling matrix compounds.

Determination of radiochemical yield and purity

To determine the actual concentration of heterodimer in the sample that needs to be labelled,
a titration was performed with [115]In, a non-radioactive isotope of ^{111}In that complexes with
chelators. A small amount of heterodimer was complexed with [115]In in different ratios.
Integrals of the complexed heterodimer peaks were used to make a calibration curve. Actual
sample concentrations were determined to be 0.54 mg/ml for compound **8a** and 0.61 mg/ml

for compound **8b**. With this concentration a more accurate determination of the radiochemical yield and purity can be made.

Radiochemical yield was measured by instant thin layer chromatography (iTLC) to have an initial indication of the purity of the labelling conditions (Figure 20). A radiochemical yield of 75% and 62% was determined for **8a** and **8b** respectively. The chromatograms show that the heterodimer seems to have insufficient conversion to move to *in vitro/in vivo* studies. A yield of at least 95% needs to be reached.
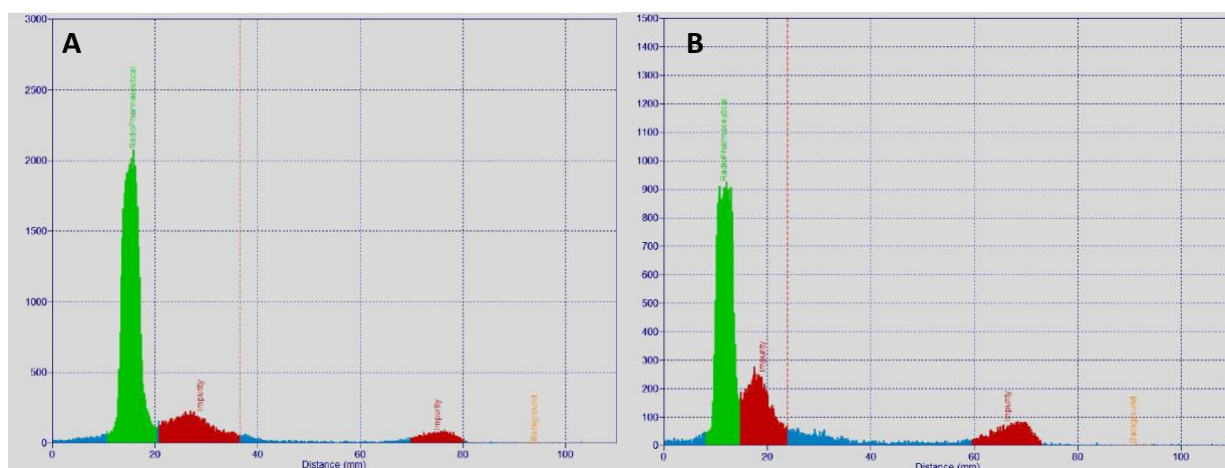
Figure 20. iTLC chromatograms (Red = Impurity/free [115]*In, Green = labelled compound*) A) iTLC chromatogram for compound **8a**. B) iTLC chromatogram for compound **8b**.

Radiochemical purity was measured by radio HPLC to establish if the insufficient values for radiochemical yield are due to conformation change or radiolysis (Figure 21). A radiochemical purity of 83% for **8a** and 51% for **8b** was determined. Due to low radiochemical yields, low radiochemical purities were also to be expected. Radiochemical purity also needs to be above 95% to continue to *in vitro/in vivo* experiments. *For 8a*, the major impurity peak was at t_R = 12.225. This is usually due to a conformation change caused by the harsh labelling conditions but could also be from radiolysis. Different labelling conditions such as lower temperatures, shorter reaction times can be used to test this. If this test results in overall lower intensity of both peaks the impurity is from radiolysis. If it results in a lower intensity of only the impurity peak conformationally changed compound. For **8b**, peak formation was seen at a shorter retention time which is usually a sign of radiolysis. However, radio-HPLC is more sensitive and can discover impurities that are not seen by LC-MS. To make sure that the peak formation during radiolabelling is indeed radiolysis, the sample should be repurified and tested for radiochemical yield and purity once more. If the impurity peaks remain the same compared

to the product peak radiolysis is confirmed but if the impurity peaks decrease compared to the product peak the sample was not pure before testing.
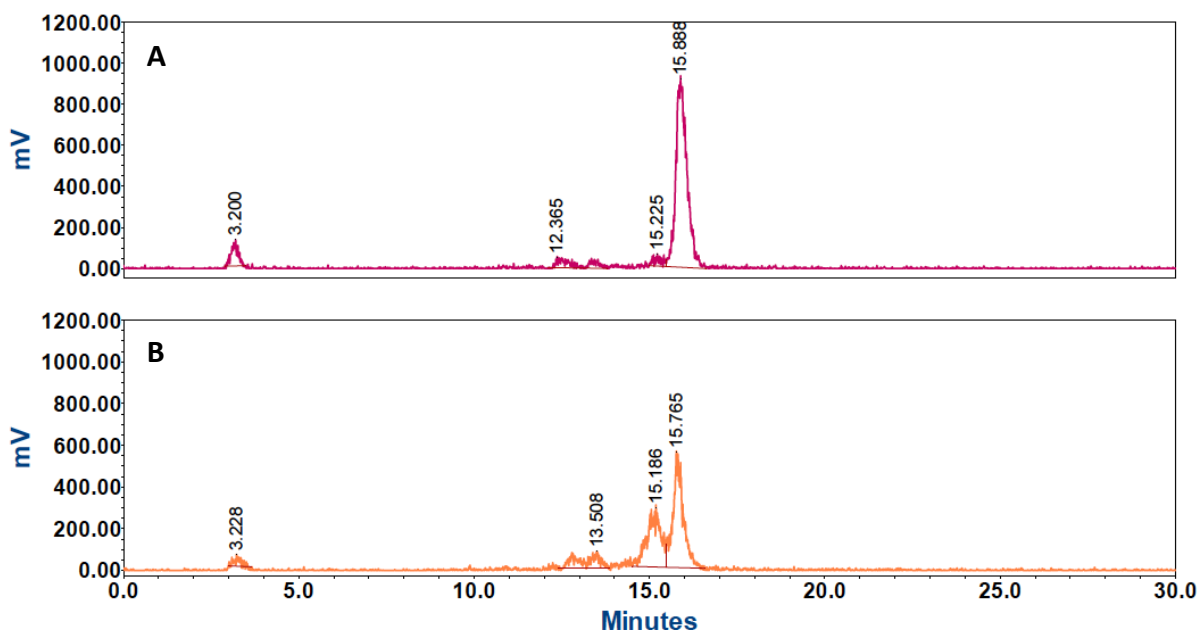
Figure 21. A) HPLC chromatogram for compound **8a**. B) HPLC chromatogram for compound **8b**.

Future perspectives

The results obtained in this research show that a GRPR and PSMA targeting heterodimer can be synthesized and is stable in aqueous environments and in the labelling matrix. Clear results for radioactive stability of the compound still remain to be gathered. First of all, the synthesized compound should be tested again on impurities. Due to the difference in sensitivity of the LC-MS and the radio-HPLC it is difficult to determine if the compound still is in the presence of impurities or if the insufficient radiochemical purity comes from radiolysis. Therefore, the compounds should be purified once more and tested on radiochemical yield and purity a second time. If the impurity peaks decrease in comparison to the product peak (increase in radiochemical yield and purity), purification methods should be revised. The time taken for the completion of the gradient is that is used in the HPLC purification method is advised to be increased in that case for better peak separation. If impurity peaks during labelling remain the same in comparison to the product peak (radiochemical yield and purity remain the same) it can be concluded that the heterodimer undergoes radiolysis and is not stable under radioactive conditions. In that case new linkers should be tested for the synthesis of the heterodimer. Disuccinimidyl suberate (DSS) and (bis[2-(succinimidyloxycarbonyloxy)ethyl]sulfone) (BSOCOES) can be potential substitutes for the PEG linkers. Both linkers have shown radioactive stability when labelled with ^{111}In and are also *in vitro* and *in vivo*.[35] The only disadvantage of using these linkers is that a thiol group needs to be added on one of the sides of the linker to be able to dimerize with the tetrazine moiety. Alternatively, the amino hexanoic acid linker on the N terminal of the peptides could be directly attached to the tetrazine giving an amine-carbon bond instead of a thiol-carbon bond.

If compounds **8a** and **8b** by the strategy proposed in this research is deemed stable result reproducibility of the synthesis scheme and stability tests should be examined. Additionally, pharmacokinetic properties of the compound should be determined. Lipophilicity, measured through LogD, can give an indication of absorption and biodistribution of the molecule. LogD can be tested through the shake-flask assay.[36] Stability of the heterodimer in PBS and mouse serum should be determined before moving to later stages. *In vitro* and ultimately *in vivo* can then be carried out. *In vitro* experiments should be carried out with PCa cells (PSMA+) and PC-3 cells (GRPR+).[18,17] Binding affinity towards PSMA and GRPR should be determined. By clicking a fluorescent dye to the tetrazine instead of the chelator, fluorescent binding assays can be used to measure binding affinity towards PSMA and GRPR independently. Moreover, it can be determined if binding affinity increases if the heterodimer is allowed to bind to a mixture of PSMA and GRPR. With a therapeutic radionucleotide attached to the heterodimer the efficacy of the heterodimer can be determined and an initial dose for *in vivo* can be calculated. *In vivo* experiments can determine biodistribution, organ uptake, efficacy of diagnostic and therapeutic capabilities in early and late stages of prostate cancer and toxicity among other pharmacodynamic and pharmacokinetic characteristics.

Conclusion

A PSMA and GRPR targeting heterodimer was successfully synthesized using a PEG_4 modified linker platform and a PEG_8 modified linker platform. It was determined that a linker platform equipped with cyanopyrimidine functionalities has stability issues when stored in aqueous environments. This is not optimal when used for clinical purposes, so a new strategy was assessed. Here an amino hexanoic linker was used to connect the peptides to the linker platform and this was deemed stable in aqueous and labelling matrix conditions for both the PEG_4 and PEG_8 modified compounds. A radiochemical yield of 75% and 62% was determined for compounds **8a** and **8b** respectively. A radiochemical purity of 83% and 51% for compounds **8a** and **8b** respectively was found, where it is still unclear if its due to radiolysis or inadequate purification.

Experimental

All chemicals were obtained from commercial suppliers and used without further purification, unless stated otherwise. All solvents were of analytical or HPLC grade and used without further purification. Reactions were magnetically stirred and monitored by thin-layer chromatography (TLC) on Merck aluminium-backed pre-coated plates (silica gel 60 F254) and visualized with ultraviolet light or by staining with ninhydrin staining. Flash column chromatography was performed on silica gel of 40-63 µm particle size. Preparative high-performance liquid chromatography (prep-HPLC) was performed on an Agilent 1290 Infinity II system equipped with an Agilent®, Prep C18 column (5 µm, 50 x 21.2 mm). Products were eluted using a gradient from 5 – 100% ACN + 0.1% Formic acid (FA) at a flow rate of 10 mL/min for 8 minutes, unless stated otherwise. Liquid chromatography-mass spectrometry (LC-MS) was carried out on an Agilent 1260 Infinity II electrospray ionisation (ESI) LC-MS system equipped with an Agilent®, InfinityLab Poroshell 120 EC-C18 column (2.7 µm, 3.0 x 100 mm). Products were eluted using gradient elution of acetonitrile (ACN; 5 – 100% in H_2O, containing 0.1% FA) at a flow rate of 0.5 mL/min for 8 minutes. Products were monitored at 220 nm, 254 nm and 280 nm by a UV detector. Radiochemical yield of radiolabeled products was carried out on a Brightspec, BSAN radio-chromatography scanner (Antwerp, Belgium). Radiochemical purity of the radiolabeled products was performed by radio-HPLC using a Waters® 2695 system (Etten-Leur, The Netherlands) equipped with a diode array detector 2998 (PDA detector) and a radioactivity detector from Canberra (Zadik, Belgium). HPLC analysis of the radiolabeled products was performed using an analytical Phenomenex (Torrance, CA, USA) Gemini RP-C18 column (5 µm, 250 x 4.60 mm) at a flow rate of 1 mL/min. The products were eluted using a gradient of acetonitrile (5 – 100 % ACN) containing 0.1% trifluoroacetic acid (TFA).

Synthesis of Boc protected amino cyanopyrimidine (1)

3-(boc-amino)propyl bromide (886 mg, 3.72 mmol), potassium carbonate (857 mg, 6.2 mmol) and sodium iodide (111 mg, 0.74 mmol) were added to a solution of 5-hydroxypyrimidine-2-carbonitrile (300 mg, 2.48 mmol) in acetone. Reaction mixture was stirred overnight at reflux. Reaction solvent was removed under reduced pressure. The final reaction mixture was purified by flash column chromatography (Hex/EtOAc = 50% - 20% Silica Gel) to afford **1** as a brown/orange oil (639.5 mg, 2.30 mmol, 93%). ^{1}H NMR (60 MHz, Chloroform-*d*) δ 8.42 (s, 2H), 4.19 (t, *J* = 6.1 Hz, 2H), 3.25 (d, *J* = 6.6 Hz, 2H), 2.07 (q, *J* = 6.0 Hz, 2H), 1.39 (s, 9H). ^{13}C NMR (15 MHz, Chloroform-*d*) δ 144.5, 77.15, 67.30, 29.73, 28.46. LC-MS *m/z* (ESI) calculated for $C_{13}H_{19}N_4O_3^+$: 279.15, found: 279.10 $[M+H]^+$.

Deprotection of Boc protected amino cyanopyrimidine (2)

1 (355 mg, 1.27 mmol) was dissolved in DCM and cooled to 0°C in an ice bath. TFA (4.02 g, 35.3 mmol) and Thioanisole (2.85 g, 23.0 mmol) were added to the cooled mixture. Reaction mixture was stirred at room temperature for 2 hours. Reaction solvent was removed under air flow. The crude was purified by reverse phase HPLC to yield **2** as a white solid (189.1 mg, 1.06 mmol, 84%). ^{1}H NMR (60 MHz, Methanol-*d*₄) δ 8.69 (s, 2H), 4.45 (t, *J* = 5.7 Hz, 2H), 3.26 (t, *J* = 6.4 Hz, 2H), 2.35 (q, *J* = 6.3 Hz, 2H). LC-MS *m/z* (ESI) calculated for $C_8H_{11}N_4O^+$: 179.10, found: 179.10 $[M+H]^+$.

Synthesis of PEG coupled cyanopyrimidine (3a, b)

The acid-PEG$_4$-thiol (20.7 mg, 73 µmol) was dissolved in DMF (2mL) after which DIPEA (37.1 mg, 0.29 mmol) and HATU (55.8 mg, 0.15 mmol) were added. The mixture was left to stir for 15 min at room temperature followed by treatment of **2** (20 mg, 0.11 mmol). The reaction was kept stirring at room temperature for another hour. Reaction solvent was removed under reduced pressure. The crude was purified by reverse phase HPLC to yield **3a** as a yellow oil (8.3mg, 19 µmol, 17%). ^{1}H NMR (60 MHz, Methanol-d_4) δ 8.72 (s, 1H), 4.40 (t, J = 6.1 Hz, 2H), 4.01 – 3.31 (m, 22H), 2.65 (dt, J = 12.0, 6.2 Hz, 3H), 2.20 (q, J = 6.3 Hz, 2H). LC-MS m/z (ESI) calculated for $C_{19}H_{31}N_4O_6S^+$: 443.20, found: 443.20 [M+H]$^+$. The same protocol was followed using the acid-PEG$_8$-thiol (53.3 mg, 0.11 mmol), **2** (20 mg, 0.11 mmol), DIPEA (58.2 mg, 0.45 mmol) and HATU (83.7 mg, 0.22 mmol) to afford **3b** as a yellow oil (4 mg, 6.7 µmol, 6%). LC-MS m/z (ESI) calculated for $C_{27}H_{47}N_4O_{10}S^+$: 619.30 , found: 618.40 [M+H]$^+$.

Synthesis of cyanopyrimidine disubstituted tetrazine platform (4a)

3a (3.3 mg, 7.5 µmol) was dissolved in ACN (0.5 mL) and added to a solution of 3, 6-Dichloro-1,2,4,5-tetrazine (0.6 mg, 3.8 µmol) and TEA (0.7 mg, 7.5 µmol) dissolved in ACN (0.5 mL). The reaction mixture was stirred at room temperature and the vials were protected from light. Reaction solvent was removed under reduced pressure. The crude was purified by HPLC to yield **4a** as a red oil (0.3mg, 0.3 µmol, 4%). LC-MS m/z (ESI) calculated for $C_{40}H_{60}N_{12}O_{12}S_2Na^+$: 985.36, found: 985.40 [M+Na]$^+$.

Synthesis of PEG disubstituted tetrazine (5a, b)

Acid-PEG$_4$-thiol (23.7 mg, 83.9 µmol) dissolved in water (7 mL) was added to 3,6-Dichloro-1,2,4,5-tetrazine (4.2 mg, 27.8 µmol) dissolved in DCM. DIPEA (22.7 mg, 0.18 mmol) was added and mixture was vortexed for 1-2 minutes. Mixture was centrifuged (4000 rpm, 4°C) and aqueous layer lyophilized. Lyophilisation yielded **5a** as a red oil (10.4 mg, 16.2 µmol, 58%). LC-MS m/z (ESI) calculated for $C_{24}H_{43}N_4O_{12}S_2^+$: 643.23, found: 643.20 [M+H]$^+$. The same protocol was followed using the acid-PEG$_8$-thiol (38.5 mg, 83.9 µmol), 3,6-Dichloro-1,2,4,5-tetrazine (4.2 mg, 27.8 µmol) and DIPEA (22.7 mg, 0.18 mmol) to afford **5b** as a red oil (12.2 mg, 12.3 µmol, 44%). LC-MS m/z (ESI) calculated for $C_{40}H_{75}N_4O_{20}S_2^+$: 995.44, found: 995.40 [M+H]$^+$.

Alternative synthesis of cyanopyrimidine disubstituted tetrazine platform (4a, b)

5a (6.5 mg, 10.1 µmol) and HATU (7.6 mg, 20.0 µmol) were dissolved in DMF (0.9 mL) and kept stirring for 15 min at room temperature. **2** was dissolved in a solution of DIPEA (5.2 mg, 40.4 µmol) and added to the reaction mixture. The reaction was left at room temperature overnight. Reaction was quenched by adding HCl and purified by reverse phase HPLC to yield **4a** as a red oil (2.5 mg, 2.6 µmol, 26%). LC-MS m/z (ESI) calculated for $C_{40}H_{60}N_{12}O_{12}S_2Na^+$: 985.36, found: 985.40 [M+Na]$^+$. The same protocol was followed using **5b** (5.6 mg, 5.6 µmol), **2** (3 mg, 16.9 µmol), HATU (4.3 mg, 11.3 µmol) and DIPEA (5.6 mg, 43.8 µmol) to afford **4b** as a red oil (2.7 mg, 2.1 µmol, 38%). LC-MS m/z (ESI) calculated for $C_{56}H_{90}N_{12}O_{20}S_2Na^+$: 1337.57, found: 1337.50 [M+Na]$^+$.

Synthesis of tetrafluorophenyl activated tetrazine platform (6a, b)

2,3,5,6-Tetrafluorophenol (10.8 mg, 65.0 μmol), EDC (10.1 mg, 65.0 μmol) and HOBt (8.6 mg, 65.0 μmol) were dissolved in 2 mL of anhydrous DMF under N_2. **5a** (10.4 mg, 16.3 μmol) was added and reaction was stirred at room temperature for 3 days while protected from light. Reaction mixture was diluted with water and washed with DCM (3 x 15 mL). Organic phase was treated with $MgSO_4$. Removing solvent under reduced pressure yielded **6a** as a red oil (8.7mg, 9.28 μmol, 58%). The same protocol was followed using **5b** (12.2 mg, 12.3 μmol), 2,3,5,6-tetrafluorophenol (8.1 mg, 49.1 μmol), EDC (7.6 mg, 49.1 μmol) and HOBt (6.6 mg, 49.1 μmol) to afford **6b** as a red oil (10 mg, 7.8 μmol, 65%). LC-MS m/z (ESI) calculated for $C_{52}H_{74}F_8N_4O_{20}S_2Na^+$: 1313.41, found: 1313.38 [M+Na]$^+$.

Synthesis of PSMA targeting ligand

The PSMA targeting ligand was synthesised using the Fmoc Solid Phase Synthesis method with 2-chlorotrityl chloride resin (100-200mesh, 1-2.5 mmol/g). Glutamic acid-Uredo moiety was synthesized in organic phase by reacting H-Glu(OtBu)-OtBu (532.5 mg, 1.8 mmol), disuccinimidyl carbonate (512.3 mg, 2.0 mmol) and TEA (174.0 mg, 1.8 mmol) in ACN. Final reaction mixture was dried and redissolved in EtOAc and then extracted with Brine and 10% citric acid to afford the protected Glutamic acid-Uredo moiety. Resin (0.66 g) was swelled in DCM (50ml, 2x15min) before loading the resin with Fmoc-Lys(ivDde)-OH (517.3 mg, 0.9 mmol) dissolved in DCM and DIPEA (290.9 mg, 2.25 mmol) by shaking for 2 hours at room temperature. Loading was checked through Nanodrop (0.2 mmol/g) The resin was capped with DCM/MeOH/DIPEA (80:15:5) for 30min at room temperature. Subsequent coupling of the amino acids Glutamic acid-Uredo moiety, Fmoc-6-Ahx-OH (283 mg, 0.8 mmol), Fmoc-L-Sta-OH (318 mg, 0.8 mmol), Fmoc-D-Phe-OH (310 mg, 0.8 mmol), Fmoc-L-Asp-OH (329 mg, 0.8 mmol) and Boc-6-Ahx-OH (185 mg, 0.8 mmol) was achieved with 4 mL HBTU (0.39 M)/Oxyma pure (0.4 M) and 2 mL DIPEA (0.8 M) and by agitating for 2 hours at room temperature. Fmoc deprotection was done by agitating the resin beads in 20% piperidine in DMF for 2x15min. ivDde deprotection was done with 5% hydrazine for 7 hours. Coupling/deprotection was checked with Nanodrop and LC-MS. The peptide was cleaved with TFA/TIPS/H_2O (95:2.5:2.5). Solution was dried and precipitated with cold Et_2O. The precipitate was purified by HPLC using a slow increasing gradient of ACN: 15%-30% for 6 min to obtain the PSMA targeting ligand as a white powder. LC-MS m/z (ESI) calculated for $C_{45}H_{73}N_8O_{15}^+$: 965.52, found: 995.50 [M+H]$^+$.

Synthesis of NeoB

The PSMA targeting ligand was synthesised using the Fmoc Solid Phase Synthesis method with 2-chlorotrityl chloride resin (100-200mesh, 1-2.5 mmol/g). Resin (66.5 mg) was swelled in DCM (5 mL, 2x15min) before loading the resin with Fmoc-His(Trt)-OH (496 mg, 0.8 mmol) dissolved in DCM/NMP (1:1) and DIPEA (258.6 mg, 2 mmol) by shaking for 2 hours at room temperature. The resin was capped with DCM/MeOH/DIPEA (80:15:5) for 30min at room temperature. Subsequent coupling of the amino acids Fmoc-L-Gly-OH (214 mg, 0.72 mmol), Fmoc-L-Val-OH (244 mg, 0.72 mmol), Fmoc-L-Ala-OH (224 mg, 0.72 mmol), Fmoc-L-Trp(Boc)-OH (379 mg, 0.72 mmol), Fmoc-L-Gln(Trt)-OH (440 mg, 0.72 mmol), Fmoc-D-Phe-OH (279 mg, 0.72 mmol) and Boc-6-Ahx-OH (254 mg, 0.72 mmol) was achieved with 1.2 mL HBTU (0.39 M)/Oxyma pure (0.4 M) and 0.6 mL DIPEA (0.8 M) and by stirring for 2 hours at room temperature. Fmoc deprotection was done by stirring the resin beads in 20% piperidine in

DMF for 2x15min. The peptide was cleaved with HFIP/DCM (2:8) for 2 x 30 min. The solution was dried and reacted overnight with 4-amino-2,6-dimethylheptane (4 eq.) in the presence of PyBOP (4 eq.) and DIPEA (8 eq.) in DMF. Reaction mixture was dried under reduced pressure and deprotected with TFA/TIPS/H$_2$O (95:2.5:2.5). After deprotection the reaction mixture was dried under reduced pressure and precipitated with cold Et$_2$O before the precipitate was subjected to purification by HPLC using a slow increasing gradient of ACN: 35%-42% for 8 min to obtain NeoB as a white powder. LC-MS *m/z* (ESI) calculated for C$_{58}$H$_{84}$N$_{13}$O$_9^+$: 1082.65, found: 1082.60 [M+H]$^+$.

Synthesis of PSMA-Tz-NeoB (7a, b)

PSMA targeting ligand (3.4 mg, 3.5 μmol) and DIPEA (0.9 mg, 7.0 μmol) were dissolved in anhydrous DMF under N$_2$. **6a** (4.4 mg, 4.6 μmol) was added to the mixture and left to stir for 30 min at room temperature while protected from the light. NeoB (5.0 mg, 4.6 μmol) was then added and mixture was left to stir for another 30 min. The final reaction mixture was purified by reverse phase HPLC using a slow increasing gradient of ACN: 35% - 42% for 8 min. Lyophilisation yielded **7a** as a red powder (2.5 mg, 0.9 μmol, 27%). LC-MS *m/z* (ESI) calculated for C$_{125}$H$_{193}$N$_{25}$O$_{34}$S$_2^+$: 2653.37, found: 2653.58 [M+H]$^+$. The same protocol was followed using **6b** (10 mg, 7.7 μmol), PSMA targeting ligand (3.8 mg, 3.8 μmol), DIPEA (0.5 mg, 3.9 μmol) and NeoB (6.3 mg, 5.8 μmol) to afford **7b** as a red oil (1.7 mg, 0.6 μmol, 15%). LC-MS *m/z* (ESI) calculated for C$_{141}$H$_{225}$N$_{25}$O$_{42}$S$_2$Na$^+$: 3027.56, found: 3027.78 [M+Na]$^+$.

Synthesis of DOTAGA-TCO

DOTA-GA anhydride (20 mg, 43.6 μmol) and TCO-amine (11.8 mg, 52.3 μmol) were dissolved in DMF (4 mL). DIPEA (28.2 mg, 218 μmol) was then added and left to stir overnight at room temperature. The final mixture was dried under reduced pressure and purified by HPLC using a slow increasing gradient of 0.01% FA in ACN: 35% - 42% for 8 min. Lyophilisation yielded DOTAGA-TCO as a white powder (17.4 mg, 25.4 μmol, 58%). LC-MS *m/z* (ESI) calculated for C$_{31}$H$_{53}$N$_6$O$_{11}^+$: 685.38, found: 685.40 [M+H]$^+$.

Attachment of DOTAGA chelator (8a, b)

7a (2.5 mg, 0.9 μmol) and DOTAGA-TCO (1.0 mg, 1.4 μmol) was dissolved in H$_2$O/ACN (1:1, 1 mL) and stirred at 37°C for 2.5 hours while protected from light. The final mixture was purified by HPLC using a slow increasing gradient of ACN: 35%-45% for 3 min. Lyophilisation yielded **8a** as a white powder (1.5 mg, 0.5 μmol, 55%). LC-MS *m/z* (ESI) calculated for C$_{156}$H$_{246}$N$_{29}$O$_{45}$S$_2^+$: 3309.73, found: 3310.18 [M+H]$^+$. The same protocol was followed using **7b** (1.7 mg, 0.6 μmol) and TCO-amine (0.6 mg, 0.85 μmol) to afford **8b** as a white powder (1 mg, 0.3 μmol, 50%). LC-MS *m/z* (ESI) calculated for C$_{177}$H$_{278}$N$_{29}$O$_{53}$S$_2^+$: 3661.94, found: 3662.38 [M+H]$^+$.

References

1.   McGuire S. World Cancer Report 2014. Geneva, Switzerland: World Health Organization, International Agency for Research on Cancer, WHO Press, 2015. *Adv Nutr*. 2016;7(2):418-419. doi:10.3945/an.116.012211

2.   Wang L, Lu B, He M, Wang Y, Wang Z, Du L. Prostate Cancer Incidence and Mortality: Global Status and Temporal Trends in 89 Countries From 2000 to 2019. *Front Public Heal*. 2022;10(February). doi:10.3389/fpubh.2022.811044

3.   Smith JA. Prevalence of prostate cancer among men with a prostate-specific antigen level =<4.0 ng per milliliter: Commentary. *Urol Oncol Semin Orig Investig*. 2004;22(6):493. doi:10.1016/j.urolonc.2004.08.008

4.   Tricoli J V., Schoenfeldt M, Conley BA. Detection of prostate cancer and predicting progression: Current and future diagnostic markers. *Clin Cancer Res*. 2004;10(12 I):3943-3953. doi:10.1158/1078-0432.CCR-03-0200

5.   Guinan P, Bhatti R, Ray P. An Evaluation of Prostate Specific Antigen in Prostate Cancer. *J Urol*. 1987;137(4):686-689.

6.   Hillier SM, Maresca KP, Femia FJ, et al. Preclinical evaluation of novel glutamate-urea-lysine analogues that target prostate-specific membrane antigen as molecular imaging pharmaceuticals for prostate cancer. *Cancer Res*. 2009;69(17):6932-6940. doi:10.1158/0008-5472.CAN-09-1682

7.   Chu E. Cancer Chemotherapy. In: *Basic and Clinical Pharmacology*. 14th ed. McGraw-Hill; 2018. doi:10.2307/j.ctv1f8xcdf.59

8.   Syn NL-X, Yong W-P, Goh B-C, Lee S-C. Evolving landscape of tumor molecular profiling for personalized cancer therapy: a comprehensive review. *Expert Opin Drug Metab Toxicol*. 2016;12:911-922.

9.   Scott AM, Allison JP, Wolchok JD. Monoclonal antibodies in cancer therapy. *Cancer Immun*. 2012;12(May):1-8.

10. Reilly RM, Sandhu J, Alvarez-Diez TM, Gallinger S, Kirsh J, Stern H. Problems of Delivery of Monoclonal Antibodies. *Clin Pharmacokinet*. 1995;28(2):126-142.

11. Marqus S, Pirogova E, Piva TJ. Evaluation of the use of therapeutic peptides for cancer treatment. *J Biomed Sci*. 2017;24(1):1-15. doi:10.1186/s12929-017-0328-x

12. Bhattacharyya S, Dixit M. Metallic Radionuclides in the Development of Diagnostic and Therapeutic Radiopharmaceuticals. *Dalt Trans J*. 2011;40(23):6112-6128. doi:10.1039/c1dt10379b.Metallic

13. Kassis AI. Therapeutic Radionuclides: Biophysical and Radiobiologic Principles. *Semin Nucl Med*. 2008;38(5):358-366.

14. Zhang Y, Guo Z, Du T, et al. Prostate specific membrane antigen (PSMA): A novel modulator of p38 for proliferation, migration, and survival in prostate cancer cells. *Prostate*. 2013;73:835-841.

15. Maurer T, Eiber M, Schwaiger M, Gschwend JE. Current use of PSMA-PET in prostate cancer management. *Nat Rev Urol*. 2016;13(4):226-235. doi:10.1038/nrurol.2016.26

16. Heynickx N, Herrmann K, Vermeulen K, Baatout S, Aerts A. The salivary glands as a dose limiting organ of PSMA- targeted radionuclide therapy: A review of the lessons learnt so far. *Nucl Med Biol*. 2021;98-99:30-39. doi:10.1016/j.nucmedbio.2021.04.003

17. Abouzayed A, Rinne SS, Sabahnoo H, et al. Preclinical evaluation of99m tc-labeled grpr antagonists masss/ses-peg2-rm26 for imaging of prostate cancer. *Pharmaceutics*. 2021;13(2):1-14. doi:10.3390/pharmaceutics13020182

18. Chang SS. Overview of Prostate-Specific Membrane Antigen. *Rev Urol*. 2004;6(10):13-

18.

19. Nock BA, Kaloudi A, Lymperis E, et al. Theranostic perspectives in prostate cancer with the gastrin-releasing peptide receptor antagonist NeoBOMB1: Preclinical and first clinical results. *J Nucl Med*. 2017;58(1):75-80. doi:10.2967/jnumed.116.178889

20. Bernhard C, Moreau M, Lhenry D, et al. DOTAGA-anhydride: Avaluable building block for the preparation of DOTA-like chelating agents. *Chem - A Eur J*. 2012;18(25):7834-7841. doi:10.1002/chem.201200132

21. Westerlund K, Honovar H, Norrström E, et al. Increasing the Net Negative Charge by Replacement of DOTA Chelator with DOTAGA Improves the Biodistribution of Radiolabeled Second-Generation Synthetic Affibody Molecules. *Mol Pharm*. 2016;13(5):1668-1678.

22. Oliveira BL, Guo Z, Bernardes GJL. Inverse electron demand Diels-Alder reactions in chemical biology. *Chem Soc Rev*. 2017;46(16):4895-4950. doi:10.1039/c7cs00184c

23. Handula M, Chen KT, Seimbille Y. Iedda: An attractive bioorthogonal reaction for biomedical applications. *Molecules*. 2021;26(15). doi:10.3390/molecules26154640

24. Yuan Y, Liang G. A biocompatible, highly efficient click reaction and its applications. *Org Biomol Chem*. 2014;12(6):865-871. doi:10.1039/c3ob41241e

25. Lockett MR, Phillips MF, Jarecki JL, Peelen D, Smith LM. A Tetrafluorophenyl Activated Ester Self-Assembled Monolayer for the Immobilization of Amine-Modified Oligonucleotides. *Langmuir*. 2008;24(1):69-75.

26. Sakate S, Kamble S, Chikate R, Rode C. Facile one-pot synthesis of aliphatic bridged diaryloxy compounds, cyclic and crown ethers under mild conditions. *Supramol Chem*. 2017;29(6):462-470. doi:10.1080/10610278.2016.1267858

27. Chen Z, Chen M, Cheng Y, et al. Exploring the Condensation Reaction between Aromatic Nitriles and Amino Thiols To Optimize In Situ Nanoparticle Formation for the Imaging of Proteases and Glycosidases in Cells. *Angew Chemie*. 2019;132(8):3298-3305.

28. Kajihara Y, Yoshihara A, Hirano K, Yamamoto N. Convenient synthesis of a sialylglycopeptide-thioester having an intact and homogeneous complex-type disialyl-oligosaccharide. *Carbohydr Res*. 2006;341(10):1333-1340. doi:10.1016/j.carres.2006.04.037

29. Andredade-Acuña D, Santos JG, Tiznado W, Cañete Á, Aliaga ME. Kinetic study on the aromatic nucleophilic substitution reaction of 3,6-dichloro-1,2,4,5-tetrazine by biothiols. *J Phys Org Chem*. 2014;27(8):670-675.

30. Tan G, Kantner K, Zhang Q, et al. Conjugation of polymer-coated gold nanoparticles with antibodies—synthesis and characterization. *Nanomaterials*. 2015;5(3):1297-1316. doi:10.3390/nano5031297

31. Brown SP, Smith AB. Peptide/protein stapling and unstapling: Introduction of s-tetrazine, photochemical release, and regeneration of the peptide/protein. *J Am Chem Soc*. 2015;137(12):4034-4037. doi:10.1021/ja512880g

32. Salvino JM, Kumar NV, Orton E, et al. Polymer-Supported Tetrafluorophenol: A New Activated Resin for Chemical Library Synthesis. *J Comb Chem*. 2000;2(6):691-697.

33. Eder M, Schäfer M, Bauder-Wüst U, Haberkorn U, Eisenhut M, Kopka K. Preclinical evaluation of a bispecific low-molecular heterodimer targeting both PSMA and GRPR for improved PET imaging and therapy of prostate cancer. *Prostate*. 2014;74(6):659-668. doi:10.1002/pros.22784

34. Liu Z, Yan Y, Liu S, Wang F, Chen X. 18F, 64Cu, and 68Ga Labeled RGD-Bombesin

Heterodimeric Peptides for PET Imaging of Breast Cancer. *Bioconjug Chem*. 2009;20(5):1016-1025.

35. Quadri SM, Vriesendorp HM. Effects of linker chemistry on the pharmacokinetics of radioimmunoconjugates. *Q J Nucl Med*. 1998;42(4):250-261.

36. Andrés A, Rosés M, Ràfols C, et al. Setup and validation of shake-flask procedures for the determination of partition coefficients (log D) from low drug amounts. *Eur J Pharm Sci*. 2015;76:181-191. doi:10.1016/j.ejps.2015.05.008